Temperature-Induced Swelling and Small Molecule Release with Hydrogen-Bonded Multilayers of Block Copolymer Micelles

Zhichen Zhu and Svetlana A. Sukhishvili*

Department of Chemistry, Chemical Biology and Biomedical Engineering, Stevens Institute of Technology, Hoboken, New Jersey 07030

ABSTRACT We report on reversible temperature-triggered swelling transitions in hydrogen-bonded multilayer films of a polycarboxylic acid and stimuli-responsive block copolymer micelles (BCMs). A neutral hydrogen-bonding temperature-responsive diblock copolymer, poly(*N*-vinylpyrrolidone)-*b*-poly(*N*-isopropylacrylamide) (PVPON-*b*-PNIPAM), was synthesized by macromolecular design *via* the interchange of xanthates (MADIX). The block copolymer exhibited reversible micellization, forming PNIPAM-core micelles with PVPON coronae in 0.01 M buffer solutions at temperatures higher than 34 °C, or in solutions with high salt concentrations ($C_{NaCl} > 0.4$ M) at 20 °C. The PVPON-*b*-PNIPAM BCMs were then assembled with poly(methacrylic acid) (PMAA) at acidic pH and higher temperature using the layer-by-layer (LbL) technique. Within the hydrogen-bonded multilayer, BCMs were stabilized through hydrogen bonding between PVPON and PMAA units and, unlike in solution, did not dissociate into unimers in low-salt solution at $T < 34$ °C. Instead, PVPON-*b*-PNIPAM BCMs reversibly swelled within film in response to temperature- or salt-concentration variations, reflecting collapse and dissolution of the BCM PNIPAM cores. The capacity of BCM/PMAA films to retain hydrophobic molecules was also dramatically dependent on temperature and/or ionic strength. The characteristic release time of pyrene from a $[BCM/PMAA]_{10}$ film decreased from 80 to 10 min upon a decrease in temperature from 37 to 20 °C. In addition, at 20 °C, ionic strength was also capable of controlling the collapse of PNIPAM micellar cores and the subsequent film swelling and pyrene release rate. Incorporation of stimuli-responsive BCM micelles within LbL films opens new opportunities in designing nanoscale films capable of controlling molecular swelling, transport, and diffusion in response to environmental stimuli.

KEYWORDS: layer-by-layer · swelling · temperature response · block copolymer micelles · hydrogen bonding · drug delivery · poly(*N*-isopropylacrylamide)

Layer-by-layer (LbL) assembly is uniquely suited for fabricating functional films with tailored composition and designed properties.[1,2] Sequential LbL deposition of polymers relies on intermacromolecular binding between assembled species, and can involve either charged or neutral polymers. Temperature is one important stimulus which can be used to control film morphology, its swelling and its capacity for delivering functional molecules. The LbL assembly of temperature-responsive multilayers has been explored in controlling the permeability of films and microcapsules. Temperature-response has often been imparted to LbL assemblies by incorporating poly(*N*-isopropylacrylamide) (PNIPAM) homopolymers or random copolymers within films. In one approach, PNIPAM was incorporated into LbL multilayers using sequential surface chemical reactions of copolymers with activated polymers containing amino or carboxylic groups.[3] Another approach is to use electrostatic interactions based on copolymers containing a PNIPAM block and a charged block to construct multilayers and capsules.[4] With cationic and anionic random copolymers of NIPAM, Jaber and Schlenoff constructed LbL films which demonstrated reversible changes in ion permeability and water content.[5] With PNIPAM microgels and cross-linker *N*,*N*′-methylene-bis-acrylamide, Lyon and co-workers immobilized microgels on glass slides and showed deswelling behaviors of microcomposite hydrogel films.[6] The same group also reported on electrostatically assembled films containing ionic temperature-responsive microgels and found that, because of the presence of extra charge within microgel particles, thermal responsiveness of such films has been hindered at neutral and basic values of pH.[7,8]

Besides electrostatically assembled films, hydrogen bonding has also been used for constructing temperature-responsive multilayers.[9] Quinn and Caruso constructed films of PNIPAM and poly(acrylic acid) (PAA), and demonstrated that at higher temperatures, such films show enhanced release rates of loaded functional molecules.[10] The same authors have also fabricated hydrogen-bonded films of poly(styrene-*alt*-maleic acid) and poly(ethylene oxide) with similarly temperature-enhanced but slower release profiles.[11] Li and co-workers demonstrated that biocompatible PNIPAM/alginate films

*Address correspondence to Svetlana.Sukhishvili@stevens.edu.

Received for review June 22, 2009 and accepted September 24, 2009.

Published online October 1, 2009.
10.1021/nn900655z CCC: $40.75

are capable of controlling the release rate of film-loaded crystalline taxol in response to temperature variations.[12] Our group has studied temperature-dependent permeability of a range of hydrogen-bonded multilayers, including poly(vinyl methyl ether) (PVME)[13] or poly(*N*-vinyl caprolactam) (PVCL)[14] with different LCSTs, and showed that PVCL/poly(methacrylic acid) (PMAA) and PVME/PMAA films exhibit temperature-responsive permeability of thymol blue dye in a temperature range from 18 to 42 °C.[15]

To enhance functionality of surface coatings, block copolymer micelles (BCMs) have recently been used as building blocks for film construction. An attractive feature of BCM-containing films is the availability of hydrophobic micellar cores which can serve as high-capacity depots for loading and release of functional hydrophobic molecules, such as drugs. Sequential assembly of BCMs with charged coronae and oppositely charged linear polyelectrolytes to form BCM-containing LbL films was described by Zhang's group.[16−18] In all these cases, BCMs consisted of glassy, nondegradable, and nonresponsive polystyrene cores and polyelectrolyte coronae. Polyelectrolyte-stabilized surfactant micelles have also been used as blocks to fabricate LbL-assembled multilayers to avoid the synthesis of block copolymers.[19] To extend the apporach to the biomedical arena, biocompatible and biodegradable micelles of poly(lactic-*co*-glycolic acid)-*b*-poly(L-lysine) were included within LbL films through sequential alternating adsorption with a polyanion.[20] In addition to BCM/polyelectrolyte constructs, BCM/BCM assembly of two types of BCMs having polycation and polyanion coronae were described by Qi *et al.*[21] and Cho *et al.*[22] The possibilty of controlling film structure and function, by combining two different types of BCMs, renders the all-BCM films attractive candidates for constructing highly functional nanostructured LbL assemblies.[23−25] Hydrogen-bonded self-assembly of biodegradable poly(ethylene oxide)-*b*-poly(ε-caprolactone) BCMs with PAA has recently been reported by Hammond and coworkers.[26] In this system, the micellar cores were not environmentally responsive, but rather the capacity of the BCM/PAA film to disintegrate at neutral pH values was utilized to deliver drug-loaded micelles from surfaces in physiological conditions. Drug release and film disintegration rates were additionally controlled by introducing cross-links between the micellar PAA blocks within self-assembled films.[26]

Incorporation of stimuli-responsive BCMs with LbL films presents an attractive means of controlling film swelling, morphology, and drug release. The advanced film functionality is enabled by the capacity of the micellar cores to be reversibly dissolved in response to environmental stimuli. Webber *et al.*[27] were first to report on monolayers of pH-responsive micelles at surfaces. These authors demonstrated reversible reconstructions of deposited monolayer of poly(2-(dimethylamino)ethyl methacrylate)-*block*-poly(2-(diethylamino)ethyl methacrylate) (PDMA-*b*-PDEA) micelles at the mica-aqueous solution interface upon pH variations. Very recently, Hammond and co-workers reported controlled release of an anticancer drug from hydrogen-bonded multilayers of BCMs and tannic acid, occurring as a result of hydrolysis of the pH-sensitive carbamate linkage between the drug and the BCM.[28] To the best of our knowledge, however, there have been no reports on multilayer films of BCMs with stimuli-responsive cores.

Micellization of PNIPAM-containing block copolymers has been extensively studied in solution.[29] Jiang *et al.*[30] reported "schizophrenic" BCM micelles of triblock copolymers comprising PNIPAM blocks. By cross-linking the shell, the micelles in solution exhibited thermal responsiveness as the result of reversible swelling and collapse of micellar PNIPAM cores. Unlike the observed reversible temperature-controlled micellization of PNIPAM-containing block copolymers, PNIPAM-grafted nanoparticles undergo reversible aggregation driven by temperature variations.[31] Here, we explore the strategy of including temperature-responsive biocompatible poly(*N*-vinylpyrrolidone)-*b*-poly(*N*-isopropylacrylamide) (PVPON-*b*-PNIPAM) BCMs within LbL films using hydrogen bonding between the PNIPAM-core/PVPON-corona micelles and a poly(carboxylic acid). We study the effect of polymeric self-assembly on temperature-response and stability of temperature-induced BCM transitions, and we show that binding with polyacid inhibited temperature-triggered dissociation of PNIPAM-core micelles to unimers. Instead, the films exhibited pronounced and reversible swelling transitions in response to temperature variations. Finally, reversible temperature or salt-controlled swelling and deswelling of BCMs in the multilayer showed dual control over release kinetics of the guest molecules, showing the capacity to retard or accelerate the diffusion of small molecules from the film.

RESULTS AND DISCUSSION

Polymer Synthesis and Characterization. *N*-vinylpyrrolidone (VPON) and its polymer PVPON are attracting considerable attention because of their solubilty in water and low toxicity. Recently, controlled radical polymerization of PVPON has been reported using the MADIX/RAFT technique.[32] The procedure is based on the use of [1-(*O*-ethylxanthyl)ethyl]benzene as an effective chain transfer agent (CTA), which is able, in the presence of AIBN, to effectively control molecular weight and the terminal group chemistry of growing PVPON chains. In this work, we used the reported procedure for the synthesis of PVPON-CTA, and then used this polymer as macro-CTA for polymerization of NIPAM to prepare PVPON-*b*-PNIPAM diblock copolymer (Scheme 1). GPC analysis in DMF revealed M_n of 19 700 with polydispersity index M_w/M_n of 1.20 for PVPON-CTA polymer, and M_n of 35 800 and M_w/M_n of 1.23 for PVPON-*b*-PNIPAM copolymer. Degree of polymerization of the PNIPAM block

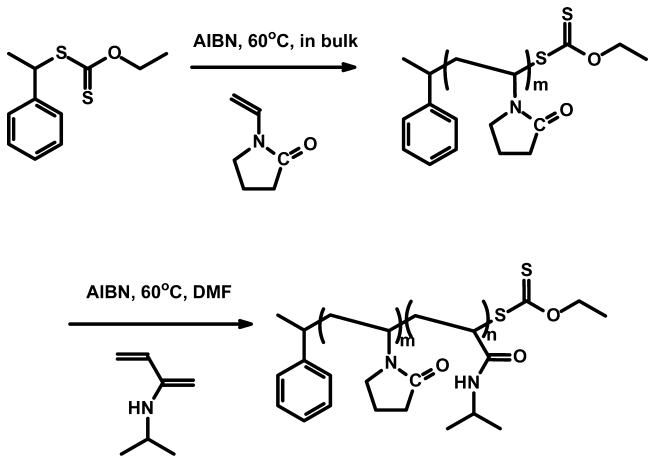

Scheme 1. Schematic representation for synthesis of $PVPON_{165}$-*b*-$PNIPAM_{140}$ diblock copolymer.

was calculated using ^{1}H NMR peak intensities and the known molecular weight of the PVPON block. Details of GPC and ^{1}H NMR characterization are described in the Supporting Information (Figures S1 and S2). The obtained block copolymer was denoted as $PVPON_{165}$-*b*-$PNIPAM_{140}$.

Stimuli-Responsive Micellization of $PVPON_{165}$-*b*-$PNIPAM_{140}$. In aqueous solution, PNIPAM homopolymers exhibit a LCST of ~32 °C.[33,34] PNIPAM chains are molecularly dispersed at temperatures below LCST and collapse in aqueous solution at temperatures above LCST. The LCST of PNIPAM is also strongly dependent on the type and concentration of small ions in solution. Binding of anions with PNIPAM units can result in an increase, but more often a decrease, in LCST with binding strength and the effect on polymer solubility following the Hofmeister series.[35−39] Therefore the micellization of PVPON-*b*-PNIPAM can be induced either by increasing solution temperature or by increasing salt concentration. In both cases, BCMs are formed with collapsed PNIPAM cores which are stabilized by PVPON coronal chains. Figure 1a shows hydrodynamic size in 0.5 mg/mL $PVPON_{165}$-*b*-$PNIPAM_{140}$ solution as a function of temperature. At room temperature, both the PVPON and PNIPAM blocks are water-soluble and the copolymers are molecularly dissolved with sizes of ~8 to 10 nm. Above 34 °C the block copolymers self-assembled into micellar aggregates with a size of ~100 nm. Micellization occurred in a narrow temperature range from 32.5 to 34 °C, and micelle size was almost constant in the temperature range from 35 to 53 °C. The CMT of $PVPON_{165}$-*b*-$PNIPAM_{140}$ block copolymer was very close to the known LCST of PNIPAM block. Figure 1b shows the hydrodynamic size in 0.5 mg/mL $PVPON_{165}$-*b*-$PNIPAM_{140}$ aqueous solution as a function of NaCl concentration at room temperature. At concentrations of NaCl below 0.35 M, the copolymers are water-soluble at room temperature with a size of ~10 nm. A drastic increase in hydrodynamic size to ~90 nm occurred in solution with NaCl concentration of 0.4 M, with only a slight further increase in size at high salt concentration.

The spherical shape of PNIPAM-core/PVPON-corona micelles was confirmed by AFM imaging of monolayer of surface-bound micelles. Figure 1c shows a contact-mode AFM image of PNIPAM-core/PVPON-corona micelles formed in solution at 45 °C and allowed to adsorb on the surface of oxidized silicon wafer at pH 2.2. The binding of BCMs at the surface of silicon wafer occurred as a result of hydrogen bonding between silanol surface groups and the carbonyl moiety of VPON rings. The average lateral size of micelles ranged from 120 to 150 nm, with average height of 65−70 nm. The larger lateral size of surface-bound micelles (as compared to their hydrodynamic size in solution of ~100 nm) reflects flattening of micelles at surfaces. Such flattening is probably induced by favorable interactions between the micellar corona and surface silanol groups, and was previously observed by others for different micellar systems.[26] Using AFM imaging, we also confirmed a spherical shape for PNIPAM-core/PVPON-corona BCMs formed in 0.5 M NaCl solution (data not shown).

Formation of BCM/Polymer LbL Films. Temperature- or salt-induced PNIPAM-core/PVPON-corona micelles were then used as building blocks for LbL assembly with PMAA. Film deposition was based on hydrogen bonding between BCM PVPON coronal chains and PMAA homopolymer units (Scheme 2). All solutions were adjusted to pH 2.2 to ensure protonation of PMAA and

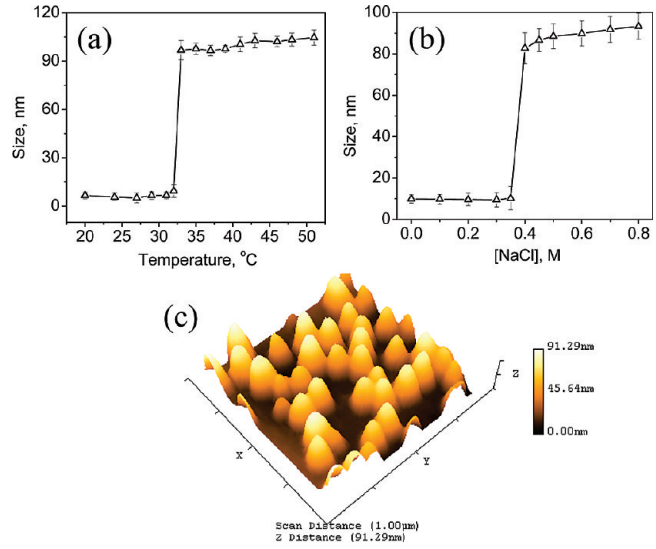

Figure 1. Hydrodynamic size in 0.5 mg/mL $PVPON_{165}$-*b*-$PNIPAM_{140}$ aqueous solution of pH 2.2 as a function of temperature (a), or as a function of concentration of sodium chloride at 20 °C (b). AFM image of a monolayer of $PVPON_{165}$-*b*-$PNIPAM_{140}$ micelles adsorbed at the surface of silicon wafer from low-salt 0.5 mg/mL $PVPON_{165}$-*b*-$PNIPAM_{140}$ solution at pH 2.2 and 45 °C (c). The sample was dried in air at 45 °C prior to AFM imaging.

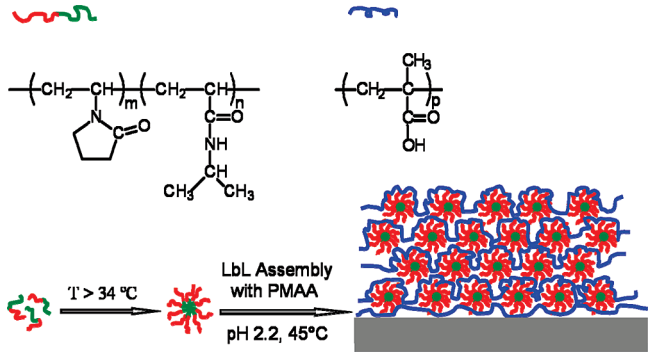

Scheme 2. Schematic illustration of $PVPON_{165}$-*b*-$PNIPAM_{140}$ micellization and hydrogen-bonded LbL assembly of BCM/PMAA multilayer films.

the existence of hydrogen bonding.[40] It was critical to keep the temperature of all deposition solutions above 34 °C so that PNIPAM chains remained collapsed within BCM cores, and the BCMs maintained their structural integrity during deposition and rinsing steps. The concentration of the BCM solution was 0.5 mg/mL, which is well above the critical micelle concentration of $PVPON_{165}$-*b*-$PNIPAM_{140}$ in aqueous solution (about 0.008 mg/mL). To enhance surface adhesion of the subsequently grown multilayers, silicon wafers or quartz slides were modified with a BPEI/PMAA bilayer as a precursor layer as described in the Experimental Section.

Figure 2a shows dependence of the dry thickness of BCM/PMAA films as a function of bilayer number. Film thickness was inferred from AFM analysis of the depth profile of the step, created by removing a portion of multilayer film from the substrate with a razor

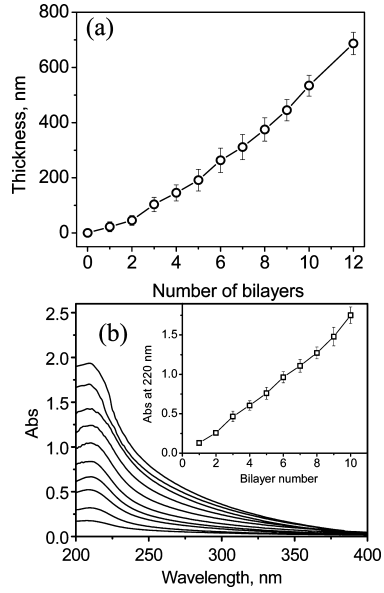

Figure 2. (a) AFM-inferred thickness of dry BCM/PMAA multilayer films deposited at the surface of silicon wafers as a function of bilayer number. (b) UV−vis spectra for BCM/PMAA film deposited at quartz slides as a function of bilayer number. Inset is absorbance *versus* the number of bilayers. Films were deposited at pH 2.2, which was first coated with ~4 nm branched polyethylenimine (BPEI)/PMAA bilayer as a precursor layer.

blade. Figure S3 in the Supporting Information shows an example of the AFM analysis of the step height using a two-bilayer film. The data in Figure 2a show that multilayer growth was linear after the third deposition cycle. In another experiment, BCM/PMAA films were deposited at the surface of quartz slide, and absorbance at 220 nm assigned to carbonyl group was used to monitor the film growth (Figure 2b).[41] The data also demonstrate a linear growth, starting from 2 bilayers, consistent with the trend in Figure 2a. From the slope in Figure 2a, a bilayer thickness after the third deposition cycle was calculated to be 54.3 nm. Among these, the thickness growth for each deposition of a PMAA layer is ~2 nm on average. The dry monolayer thickness per BCM layer in the linear region was twice as small as the hydrodynamic size of hydrated micelles of ~100 nm, reflecting dehydration of BCMs after deposition at surfaces. AFM images in Figures 1c and 3a indicate that for a first bilayer deposited, silicon substrates were not completely covered with BCMs. The ellipsometric thickness of a dry monolayer of BCMs was 20.9 ± 4.2 nm. An initial nonlinear growth followed by linear growth curve was also reported for electrostatically fabricated LbL films.[42] In contrast to this reported data, PNIPAM-*b*-PVPON micelles are neutral and lack electrostatic repulsion between charged coronae. The incomplete surface coverage in the case of PNIPAM-core/PVPON-corona micelles is probably associated with a lack of micellar mobility at the surface, which is required for the formation of highly packed micelle monolayer. Indeed, as micelles are randomly adsorbed at the surface, adsorption of later-arriving micelles is inhibited because of the insufficient size of landing spots remaining in between surface-bound micelles. These "defects" were filled as subsequent layers of PMAA and BCMs were deposited at the surface, and for a three-bilayer film the surface was fully covered by BCMs (Figure 3b). For thicker films, AFM images of dry films show dense deposition of micelles at film surfaces (Figure 3c,d). The root-mean-square (rms) roughness of the BCM/PMAA films increased with the number of bilayers, and leveled off at a value of 54 ± 5 nm for films thicker than 6 bilayers. In particular, the rms roughness of 1-, 3-, 6-, and 10-bilayer BCM/PMAA films was 24.0, 32.4, 57.1, and 50.8 nm, respectively. The limiting value of rms roughness of 54 ± 5 nm is close to the average bilayer thickness in the linear film growth region of 54.3 nm. In this regime, BCMs are adsorbed onto a quasi-3D surface with a constant roughness, and a constant number of micelles are deposited at surfaces per deposition cycle, resulting in linear multilayer growth shown in Figure 2.

BCM/PMAA multilayers were stable at pH values below 6.2 and could be erased from the surface by exposure to solution at higher pH values. Such behavior is consistent with our earlier findings of dissolution of PVPON/PMAA films at pH 6.9.[43] The slightly lower criti-

cal dissolution pH value for BCM/PMAA films is probably due to steric instability of coronal PVPON chains to conform to PMAA chains.

Temperature Response of BCM Films—From Monolayers to Multilayers. We then aimed to explore whether the temperature-triggered behavior of surface-bound micelles differed from their micellization in solution. Figure 4a,b shows AFM images of a monolayer of adsorbed BCMs as deposited from phosphate buffer of pH 2.2 at 45 °C (Figure 4a) and after exposure to the same buffer solution at room temperature (Figure 4b). Figure 4c also shows an example of a similar exposure of the BCM/PMAA bilayer to a solution with temperature below LCST. All substrates were dried at 45 °C in air before AFM imaging. With no PMAA layer on the top, the BCM monolayer disintegrated in low-temperature solution, as seen from the morphological changes in Figure 4b. The ellipsometric thickness of dry BCM monolayer shown in Figure 4 panels a and b decreased from 20.9 ± 4.2 nm to 5.7 ± 2.0 nm, respectively, indicating desorption of a significant fraction of PNIPAM-*b*-PVPON chains into solution. The mass loss and morphological changes were irreversible with temperature change. In work by others, environmentally triggered dissociation of a surface-adsorbed BCM monolayer was studied,[27] and the degree of reversibility of pH-triggered morphological changes was shown to be dependent on the strength of binding between coronal chains and substrate functional groups. Specifically, reversible or irreversible dissolution of a surface-bound micelle monolayer was observed for mica or oxidized silicon wafer surfaces, respectively.[27] We suggest that in our case the strong binding between PVPON coronal chains and surface silanol groups results in irreversibility of temperature-triggered morphological changes of adsorbed BCM monolayer. In addition, readsorption of all PNIPAM-*b*-PVPON chains at the surface after temperature-triggered micellar disintegration was not possible because of the prohibitively high mass of the PNIPAM-*b*-PVPON chains within the BCM monolayer.

In drastic contrast, the BCM/PMAA bilayer maintained its original dry mass and structural integrity for surface-coated micelles when exposed to solution with temperature below LCST (Figure 4c). With a PMAA top layer, the thickness of a one-bilayer film remained 22.3 ± 3.9 nm before and after exposure to solution at room temperature. Moreover, we have immersed one-bilayer BCM/PMAA films in phosphate buffer of pH 2.2 at room temperature for as long as 96 h, and found no changes in micellar morphology or in the micellar surface coverage. This suggests that a coating of hydrogen-bonding PMAA chains on PNIPAM-core/PVPON-corona micelles inhibited temperature-triggered dissolution of BCMs. AFM data also suggest that stabilization of PNIPAM-core/PVPON-corona micelles at the film surface at room temperature occurred for BCM/PMAA films of various thicknesses (*e.g.*, 3-, 6-, and 10-bilayer films) with PMAA deposited as the top layer. This result shows a facile way of stabilization against temperature variation for otherwise dissolvable micelles *via* self-assembly with a homopolymer at surface.

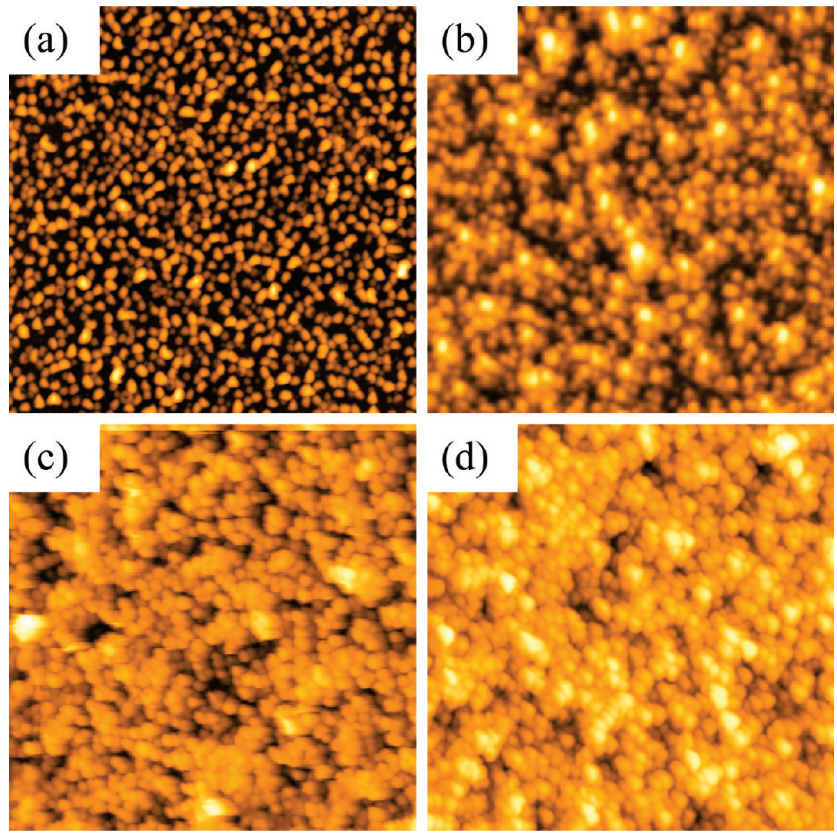

Figure 3. AFM images of dry [BCM/PMAA]$_n$ films as a function of bilayer number *n*: *n* = 1 (a), *n* = 3 (b), *n* = 6 (c), and *n* = 10 (d). Their root-mean-square roughness is 24.0, 32.4, 57.1, and 50.8 nm, respectively. Films were deposited from solutions of pH 2.2 at 45 °C and dried in air at 45 °C. In all images, the scanned area was 5 μm × 5 μm. All silicon wafers were coated with a BPEI/PMAA bilayer as a precursor layer.

Temperature-Triggered Swelling of BCM/PMAA Films. We then aimed to explore whether temperature-induced phase transitions within PNIPAM cores of self-assembled BCMs can be used to control the extent of film swelling. To that end, we fabricated a [BCM/PMAA]$_4$ film with a dry thickness of 140 ± 17 nm and applied *in situ* ellipsometry to monitor film swelling as a function of temperature in aqueous solution. A [BCM/PMAA]$_4$ film was used for *in situ* ellipsometry, as its thickness is most suitable for simultaneous determination of thickness and refractive index.[44] These experiments were performed in 0.01 M phosphate buffer of pH 5.0. This pH is lower than the critical disintegration pH of BCM/PMAA films at 6.2, and BCM/PMAA films are

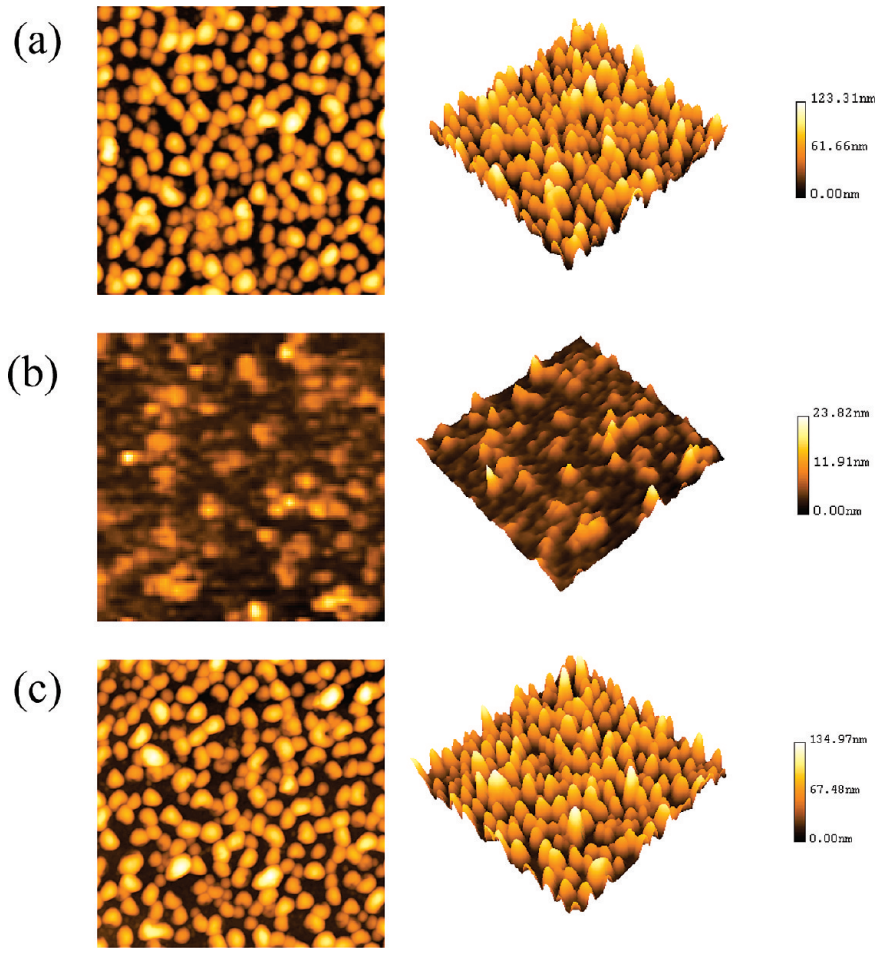

Figure 4. AFM images of a monolayer of PVPON-*b*-PNIPAM micelles deposited from 0.01 M phosphate buffer of pH 2.2 at 45 °C at the silicon wafer surface before (a) and after (b) exposure to phosphate buffer of pH 2.2 at 20 °C. AFM image of a $[BCM/PMAA]_1$ film after exposure to phosphate buffer of pH 2.2 at 20 °C overnight (c). All films were dried in air at 45 °C before AFM imaging. In all images, the scanned area was 2 μm × 2 μm. All silicon wafers were first coated with a BPEI/PMAA bilayer as precursor layer.

stable because of sufficiently extensive hydrogen bonding between protonated PMAA chains (pK_a value of PMAA is reported to be ~6 to 6.8[45]) and the PVPON chains in the micellar corona. An ellipsometry cell containing silicon substrate deposited with a $[BCM/PMAA]_4$ film was filled with 0.01 M phosphate buffer of pH 5.0, and measurements were performed after the temperature was allowed to equilibrate for 10 min. Figure 5 panels a and b show the temperature dependence of thickness and refractive index for a $[BCM/PMAA]_4$ film. At 20 °C, an average film thickness of 230 ± 15 nm, and a low refractive index of 1.365 suggests a significant swelling of the multilayer film (swell ratio of 1.60−1.65). When the solution temperature was elevated to 45 °C, the film thickness decreased to 156 ± 10 nm (swell ratio of 1.10−1.16), and its refractive index increased to 1.405, suggesting deswelling of the film resulting from the collapse of the PNIPAM-core polymer chains of hydrogen-bonded micelles. Theoretically, a single polymer chain will swell in order to maximize the number of polymer-fluid contacts in good solvent. If we assume a PNIPAM chain behaves as Gaussian chain in aqueous solution at 20 °C, the radius of gyration for the $PNIPAM_{140}$ chain was estimated to be ~6 nm. As temperature increases to 45 °C, the $PNIPAM_{140}$ chain behaves like a solid sphere in bad solvent, undergoing a coil-to-globule transition. With the assumption of a density of 1.0 g cm^{-3} for the collapsed polymer sphere, the radius of the hard globule at 45 °C is calculated to be ~2 nm. The theoretical ratio of these radii at 3.0 reveals a change of the $PNIPAM_{140}$ chain conformation in water with an increase in temperatures. The measured value of swelling ratio of 1.60 is twice as small as the calculated value of 3 because the surrounding matrix of the PVPON shell and PMMA layer makes up more than half of the composite mass and exhibits no change of conformation with temperature. Figure 5c shows an AFM image of the same area after the film was dried at 45 °C and Figure 5d shows the wet film at 20 °C. For a film soaked with water at 20 °C, swollen micelles were clearly observed with sizes of ~180 to 220 nm (Figure 5d), while micellar size was ~100 to 120 nm for film dried at 45 °C (Figure 5c). The corresponding root-mean-square roughness of the wet and dry films shown in Figure 5 panels c and d was 19.7 and 34.3 nm, respectively. Remarkably, film swelling/deswelling was largely reversible even after four swelling cycles. The film swelling/deswelling occurred as a result of temperature-induced collapse or dissolution of PNIPAM cores of self-assembled BCMs. The transition is reversible due to stabilization of BCMs within LbL films achieved by hydrogen-bonding with PMAA chains. These results indicate that while hydrogen-bonded within multilayer films, PNIPAM-core micelles retain the LCST behavior that enables temperature control over film swelling. Earlier experiments by others demonstrated that electrostatic repulsion within poly(NIPAM-*co*-acrylic acid) microgels resulted in the loss of temperature responsiveness for microgel-containing LbL films.[8] Our system lacks these potentially inhibiting electrostatic interactions and is therefore advantageous over systems which employ charged copolymers of NIPAM.[5,8] Finally, it is important that a simple noncovalent self-assembly of PMAA homopolymer with PNIPAM-core/PVPON-corona micelles results in robust films that show revers-

ible temperature-induced swelling transitions. The reversibility of such transitions is assured by strong hydrogen bonding between PVPON coronae and PMAA homopolymer units.

Effect of Temperature on Release of Pyrene from BCM/PMAA Multilayers. We then explored whether temperature-controlled collapse/swelling transitions in self-assembled BCM PNIPAM cores could be used to control the release rate of hydrophobic functional molecules. Pyrene, a small hydrophobic molecule, was used as the model molecule. With the expectation that poorly water-soluble pyrene can be incorporated within BCM/PMAA films at temperatures above PNIPAM's LCST where micellar PNIPAM cores are collapsed, pyrene dye was loaded into $[BCM/PMAA]_{10}$ films using saturated pyrene solution of pH 5.0 at 45 °C as described in the Experimental Section. Fluorescence spectrum of pyrene-loaded film is shown in Figure S4. To avoid desorption of loaded pyrene from the film, spectrum was taken immediately after immersing the pyrene-loaded BCM/PMAA film into pH 5.0 solution at 45 °C. From Figure S4, we calculated ratio of the fluorescence intensities at 373 and 383 nm, I_{373}/I_{383}, as 0.92. This value indicates that pyrene was included into the hydrophobic environment of film.[46] Note that the I_{373}/I_{383} intensity ratio in pyrene-loaded BCM/PMAA multilayer films was lower than that of ~1.10 for solution of BCMs at elevated temperatures. The difference in intensity ratios between pyrene-loaded micelle solution and dry multilayer films were also reported by others.[16] We suggest that the lower I_{373}/I_{383} ratio of pyrene fluorescence within multilayer films as compared with the BCM solution is attributed to a more hydrophobic environment within the film resulting from dehydrated hydrogen-bonded PMAA and PVPON coronal chains. Indeed, hydrogen-bonding polymers will collapse from solution upon formation of interpolymer complexes, and poly(carboxylic acid) chains contract as a result of hydrogen bonding with neutral polymers.[47] To differentiate loading of pyrene dye between collapsed micellar PNIPAM cores and hydrophobic PVPON-corona/PMAA matrix, we conducted a controlled experiment in which pyrene dye was loaded into a model film built from homopolymers of PVPON and PMAA. Pyrene release experiments were all conducted on 1.4 × 2 cm^2 quartz slides deposited with $[BCM/PMAA]_{10}$ or $[PVPON/PMAA]_{10}$ films immersed in 30 mL of pH 5.0 buffer solution. Figure 6 shows that a much larger amount of pyrene was released from the $[BCM/PMAA]_{10}$ film during first extraction compared to the control $[PVPON/PMAA]_{10}$ film. Loaded pyrene dye was then extracted from films with fresh buffer solution several times until completion. Inset in Figure 6 shows that while ~90% of pyrene was released from $[PVPON/PMAA]_{10}$ film after first extraction, multiple extractions were needed to release all pyrene from $[BCM/PMAA]_{10}$ film. The pyrene loading capacity of films was calculated from the cumulative amount of pyrene released to solution after multiple extraction cycles. Importantly, BCM-containing films were capable of loading and releasing 25 times more dye than $[PVPON/PMAA]_{10}$ film. The result confirms that dye loading and release is pri-

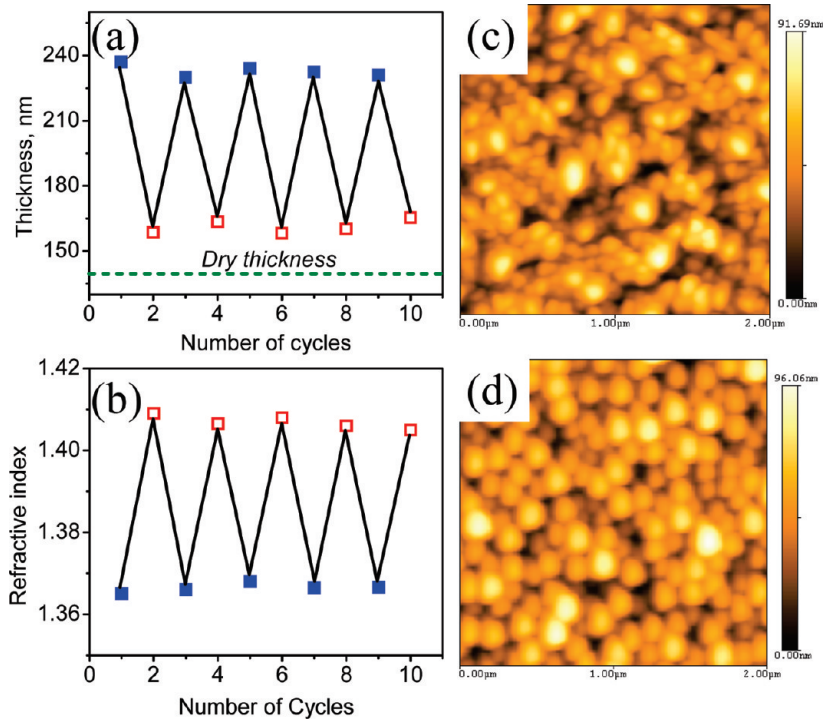

Figure 5. *In situ* ellipsometry measurements of thickness (a) and refractive index (b) of a $[BCM/PMAA]_4$ film in 0.01 M phosphate buffer of pH 5.0 at 20 °C (filled squares) and 45 °C (open squares), and AFM images taken for film dried at 45 °C (c) as well as for wet film at 20 °C (d).

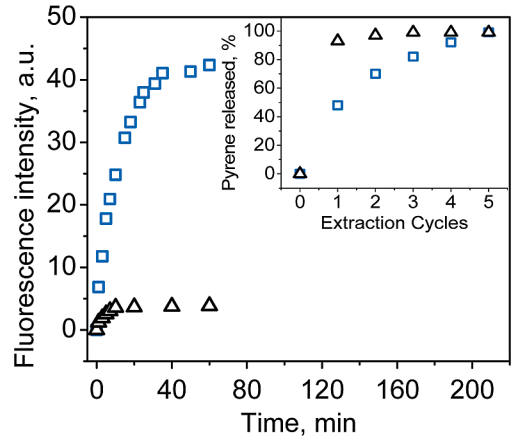

Figure 6. Release profiles of pyrene from a $[BCM/PMAA]_{10}$ film (squares) and a $(PVPON/PMAA)_{10}$ film (triangles) as inferred from fluorescence measurements at λ_{ex} = 338 nm and λ_{em} = 373 nm. Pyrene release was conducted in 30 mL of 0.01 M phosphate buffer of pH 5.0 at 20 °C. Inset shows the total percentage of pyrene released from films after multiple extraction cycles.

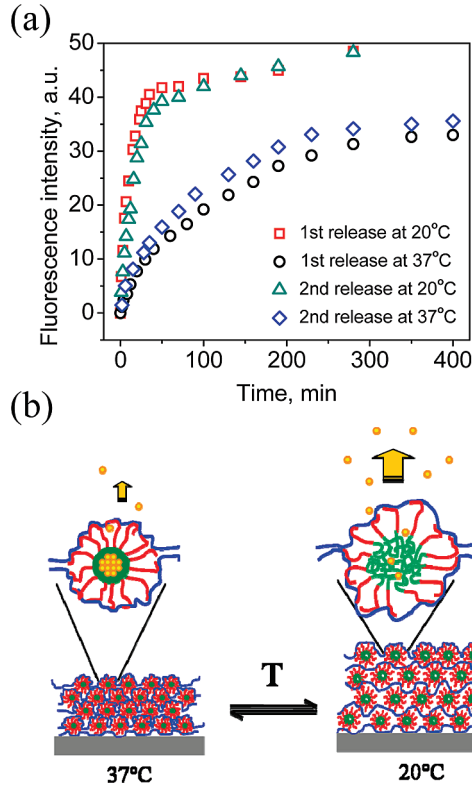

Figure 7. (a) Release kinetics of pyrene from a $[BCM/PMAA]_{10}$ film in 30 mL of pH 5.0 buffer solution at 20 and 37 °C. Pyrene release was monitored by measuring fluorescence intensity of pyrene accumulated in solution (λ_{ex} = 338 nm, λ_{em} = 373 nm). (b) Schematic representation of reversible temperature-triggered swelling of BCM/PMAA films.

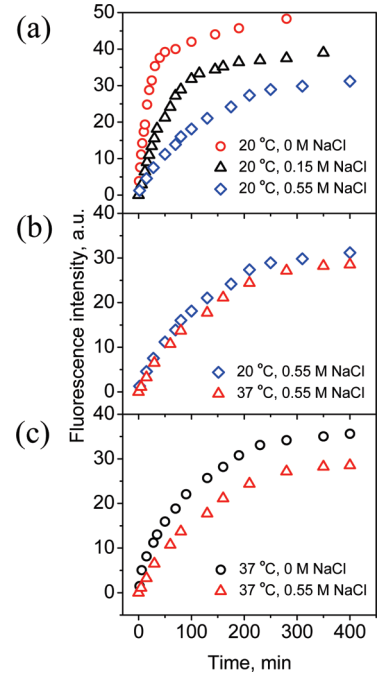

Figure 8. Release profiles of pyrene from a $[BCM/PMAA]_{10}$ film (a) at 20 °C with different NaCl concentrations; (b) in 0.55 M NaCl solution with two temperatures; (c) at 37 °C with 0 and 0.55 M NaCl solutions. All release experiments were conducted in 0.01 M phosphate buffer of pH 5.0.

marily due to micellar PNIPAM cores. From the overall fluorescence intensity of pyrene released to solution from $[BCM/PMAA]_{10}$ film, we calculated the amount of pyrene loaded within the 1.4 × 2 cm^2 $[BCM/PMAA]_{10}$ film to be 0.18 μg/cm^2. This value corresponds to 3.7 × 10^{-12} μg pyrene or 1.1 × 10^3 pyrene molecules per micelle.

Figure 7 shows the release profiles of pyrene from a $[BCM/PMAA]_{10}$ film immersed in 0.01 M phosphate buffer of pH 5.0 at two different temperatures of 20 or 37 °C. At 37 °C, pyrene was released over a span of 4 h (the characteristic release time at which 50% of pyrene was released was at 80 min). A similar release experiment at a lower temperature of 20 °C showed a much faster release in 1 h (50% released at 10 min). The difference in release time is evidently due to thermoresponsive behavior of PNIPAM micellar cores. At temperatures above PNIPAM's LCST, pyrene was more strongly retained by the collapsed hydrophobic BCM PNIPAM cores, and the redistribution kinetics between the hydrophobic micellar and aqueous phase was slow. At room temperature, when the PNIPAM core in self-assembled BCMs swelled and absorbed large amounts of water, release of pyrene molecules occurred faster. The release mechanism was also analyzed from plots of log $M(t)/M(\infty)$ against log t, where M is the amount of pyrene released, $M(t)/M(\infty)$ is the fraction of pyrene released at time t, and $M(\infty)$ the total amount of pyrene in loaded film. The plots of pyrene release are shown in Figure S5. The calculated slopes for the multilayer film were 0.65 and 0.48, at 20 to 37 °C, respectively. These values show that while at 37 °C, the dye is released from the film by Fickian diffusion ($n < 0.5$),[48] the release becomes non-Fickian ($0.5 < n < 1$)[48] at 20 °C as dye dissociates from the PNIPAM chains which become hydrophilic at this temperature.

Effect of Salt on Release of Pyrene from BCM/PMAA Multilayers. As shown in Figure 1b above, collapse of PNIPAM chain in PVPON-*b*-PNIPAM block copolymer can also be induced at room temperature by increasing concentration of sodium chloride. At high salt concentrations, binding of anions to PNIPAM unit results in chain dehydration, and "salted-out" PNIPAM chains segregate into the micellar core.[39] PNIPAM-core micelles with size of ~90 nm exist at concentrations of NaCl higher than 0.4 M. We then aimed to explore whether ionic strength can cause a similar collapse of PNIPAM blocks of micelles within BCM/PMAA multilayers, and whether such a collapse can affect the release rate of micelle-loaded dye. BCM/PMAA films were produced and loaded with pyrene dye at high temperature, and the loaded dye was then allowed to release from film into solution with different NaCl concentrations. Figure 8a compares pyrene release rates at several concentrations of salt. In buffer solutions at 20 °C and with no additional sodium chloride, the release rate was relatively fast, with a short span of 1 h (50% released at 10 min). A similar result has been shown in Figure 7. The fast re-

lease rate results from decreased retention of pyrene by the hydrated, hydrophilic PNIPAM chains. In buffer solution containing 0.15 M NaCl, a significant decrease of the release rate occurred in a sustained manner over 2 h (50% released at 35 min), and the amount of released dye was smaller. Interestingly, this effect was observed despite the fact that at this salt concentration PNIPAM chains were not yet completely dehydrated. Finally, in solution with 0.55 M NaCl, release of pyrene was further slowed down, with release occurring over a span of 5 h (50% released at 120 min). This deceleration of dye diffusion from the film is a result of stronger partitioning of dye in collapsed hydrophobic micellar PNIPAM cores. Such effect of salt on dye release is very different from the previously demonstrated ionic-strength-triggered loosening of polystyrene micellar cores within electrostatically assembled multilayer films of a polycation and polystryrene-*b*-poly(acrylic acid) BCMs, and resultant faster release of pyrene from the film.[16] Also note that thermally induced structural transitions in polyelectrolyte multilayers as a result of thermally induced breakage of ionic pairs have been reported earlier.[49] In our case, swelling transitions in multilayer occurred as a result of temperature- or salt-induced collapse or dissolution of PNIPAM cores of assembled BCMs.

We then aimed to compare the magnitudes of the effects of temperature and salt on dye retention and release. Figure 8b shows that release rates of pyrene from the BCM/PMAA film were comparable in 0.55 M NaCl solution at 20 and 37 °C. However, for the same temperature of 37 °C, dye was more strongly retained within film when exposed to solution with 0.55 M NaCl (Figure 8c). The data reflect a synergistic effect of temperature and salt on dehydration of PNIPAM chains and show that even at temperatures above LCST where PNIPAM chains are collapsed, further chain dehydration occurs in salt solution. Indeed, it has been reported that collapsed PNIPAM cores may contain as much as 80% water.[50] The similarity of pyrene release rates in Figure 8b is likely due to the offsetting effect of increased chain hydrophobicity by the fundamentally faster diffusion rate at higher temperatures.

CONCLUSION

We report here on environmentally responsive hydrogen-bonded multilayer films which are fabricated using neutral diblock copolymer micelles as building blocks. Self-assembly of environmentally responsive BCM with a polycabroxylic acid using hydrogen-bonding self-assembly results in stabilization of BCMs toward dissociation. The assemblies exhibit reversible swelling transitions and are capable of controlling the release rate of an incorporated hydrophobic dye in response to variations in temperature or salt concentration. The maintenance of structural integrity of assembled micelles is essential for loading functional molecules, and, by tailoring the size of the micellar core, might allow further control over the loading capacity. A combination of the structural integrity of stabilized BCM with the film's capacity for reversible swelling in response to temperature variations makes BCM/poly(carboxylic acid) multilayers excellent candidate for future controlled delivery and microfluidic device applications.

EXPERIMENTAL SECTION

Materials. *N*-vinylpyrrolidone (VPON) (Aldrich, >99%) was distilled twice under reduced pressure to remove inhibitors. *N*-isopropylacrylamide (NIPAM) (Aldrich, 97%) was purified twice by recrystallization from a mixture of hexane and benzene (7/3, v/v). α,α-Azobis(isobutyronitrile) (AIBN) (Aldrich, 98%) was purified by recrystallization from methanol. *N*,*N*-Dimethylformamide (DMF) (Aldrich, 99%) was freshly distilled under reduced pressure before use. [1-(*O*-Ethylxanthyl)ethyl]benzene was prepared according to the literature.[32] Millipore (Milli-Q system) water with a 18.2 MΩ cm^{-1} resistivity was used. BPEI with M_w = 25 kDa, PMAA with M_w = 150 kDa, hydrochloric acid, sodium hydroxide, sodium chloride, and dibasic and monobasic sodium phosphate were purchased from Sigma-Aldrich. All other reagents were purchased from Sigma-Aldrich and used as received.

Synthesis of PVPON-*b*-PNIPAM Diblock Copolymers. ***Homopolymerization of VPON by MADIX.*** VPON (8.88 g, 80 mmol), [1-(*O*-ethylxanthyl)ethyl]benzene (120.8 mg, 0.53 mmol), and AIBN (17 mg, 0.11 mmol) were mixed in a glass ampule with a magnetic stirring bar. The solution was degassed by three cycles of freeze-vacuum−thawing, and then sealed under argon atmosphere. The polymerization was carried out at 60 °C for 12 h. The mixture was diluted with methanol and precipitated into a large amount of anhydrous diethyl ether three times. The product was collected by filtration and dried at room temperature for 24 h. The gravimetrically determined product yield was 62%.

Block Copolymerization of NIPAM. The obtained PVPON contained an ethylxanthyl group at its terminus and has been used as macromolecular chain transfer agent (macro-CTA) for the synthesis of PVPON-*b*-PNIPAM block copolymer. A representative procedure was as follows: PVPON macro-CTA (1.832 g, 0.1 mmol), AIBN (2.2 mg, 14 mmol), and NIPAM (1.695 g, 15 mmol) were mixed in DMF (4 mL), and the solution was degassed by three freeze-vacuum−thawing cycles and sealed under argon atmosphere. The polymerization was carried out at 60 °C for 18 h. The product was purified by precipitation from chloroform into a large amount of diethyl ether three times. The product was collected by filtration and dried at room temperature for 24 h. The gravimetrically determined product yield was 70%.

Characterization Techniques. ***NMR Spectroscopy.*** All ^{1}H NMR spectra were recorded using a Varian Inova 400-MHz NMR spectrometer in D_2O at room temperature.

Gel Permeable Chromatography (GPC). Molecular weights and molecular weight distributions were determined by GPC using two linear Styragel columns HT3 and HT4 and a column temperature of 35 °C. Waters 1515 pump and Waters 2414 differential refractive index detector (set at 30 °C) was used. The eluent was DMF at a flow rate of 1.0 mL/min. To determine number average molecular weights M_n and molecular weight distributions M_w/M_n for the sample polymers, chromatographic columns have been calibrated with standard polystyrene samples.

Dynamic Light Scattering. Hydrodynamic sizes in block copolymer solution were measured using Zetasizer Nano-ZS equipment (Malvern Inc.).

Atomic Force Microscopy (AFM). AFM measurements were performed in air using NSCRIPTOR Dip Pen Nanolithography system (Nanoink). For AFM imaging, micelles were deposited on silicon wafers by drying BCM-containing solution at 45 °C.

Ellipsometry Measurements of Dry and Swollen Films. The thicknesses of dry and swollen BCM/PMAA films were measured by a home-built phase-modulated ellipsometer at 65° angle of incidence.[44] Optical properties of the substrates and oxide layer thickness were determined prior to polymer deposition. In the case of dry polymer films, the refractive index was fixed at a value of 1.5.

Measurements of the swelling of BCM/PMAA films were performed *in situ* using a custom-made cylindrical flow-through quartz cell. To obtain swollen film thickness, the cell was filled with 0.01 M phosphate pH 5.0 buffer solution at different temperatures, and measurements were taken after a minimum equilibration time of 10 min.

Multilayer Deposition and Dye Loading and Release. ***Preparation of Block Copolymer Micelles (BCMs).*** Above the critical micellization temperature (CMT) of 34 °C, the block copolymer PVPON-*b*-PNIPAM self-assembled into PNIPAM-core micelles. A typical procedure to prepare BCMs is as follows: 20 mg block copolymer PVPON-*b*-PNIPAM was dissolved into 40 mL of 0.01 M phosphate buffer of pH 2.2. The solution was heated to 45 °C, when BCMs were formed. The presence of micelles in PVPON-*b*-PNIPAM solution at temperatures higher than 34 °C was confirmed by AFM.

Deposition of a Precursor Layer. Silicon wafers or quartz slides were cleaned as described elsewhere.[45] To enhance surface adhesion of subsequently grown multilayers, substrate was coated with BPEI/PMAA bilayer as a precursor layer. BPEI and PMAA solutions used in precursor deposition were prepared in 0.01 M phosphate buffer of pH 5.5; the same buffer solution was used for rinsing steps. Silicon wafers or quartz slides were alternately exposed to 0.2 mg/mL BPEI and PMAA solution for 10 min, with two 1-min rinsing cycles in buffer solution between polymer deposition steps. The substrates with deposited BPEI/PMAA precursor film were rinsed in Milli-Q water and used for construction of BCM/PMAA multilayer films.

Deposition of BCM/PMAA Multilayers. All deposition and rinsing steps were performed in 0.01 M phosphate buffer of pH 2.2 at 45 °C. Hydrogen-bonded BCM/PMAA multilayers were deposited by alternately exposing the substrate to BCM and PMAA solution for 15 min with two 1-min intermediate rinsing steps with 0.01 M phosphate buffer. Multilayer construction started with exposing the precusor-coated substrate to BCM solution in a 0.01 M phosphate buffer of pH 2.2 at 45 °C and continued until the desired number of bilayers *n* was deposited. The produced $[BCM/PMAA]_n$ films were dried in air at 45 °C.

Dye Loading and Release. For all loading and release experiments, we used a $[BCM/PMAA]_{10}$ film. Specifically, quartz substrates with $[BCM/PMAA]_{10}$ films were immersed in 100 mL of pyrene-saturated 0.01 M phosphate buffer of pH 5.0 at 45 °C for 4 h. The loading monitored by fluorescence spectra of film showed that loading capacity reached the maximum in 3 h under these conditions (Figure S4). Fluorescence intensity at $\lambda_{em} = 391$ nm was used to monitor the loading of pyrene dye. The wafers were then rinsed three times with 0.01 M phosphate buffer of pH 5.0 (1 min for each rinse) and dried in air at 45 °C. Pyrene release experiments were all conducted in pH 5.0 buffer solution. Specifically, a 1.4×2 cm^2 quartz slide deposited with $[BCM/PMAA]_{10}$ film was immersed in 30 mL of buffer solution under different conditions. Aliquots (3 mL) of the buffer solutions were taken at time intervals to determine the rate of pyrene release. Fluorescence intensity at $\lambda_{em} = 373$ nm was used to measure the pyrene accumulated in solution. When the released pyrene reached equilibrium, the buffer solution was replaced with 30 mL of fresh buffer solution to continue the release. Multiple extractions with fresh buffer solutions were carried out until the loaded pyrene dye was completely released.

Acknowledgment. This work was supported by the National Science Foundation (Award DMR-0710591). We thank Thomas Cattabiani (Stevens Institute of Technology) for help with preparation of the manuscript.

Supporting Information Available: GPC and ^{1}H NMR characterization of PVPON-*b*-PNIPAM copolymer; AFM analysis of the dry film thickness; fluorometry of pyrene-loaded BCM/PMAA films; analysis of kinetics of pyrene release from BCM/PMAA films; additional figures. This material is available free of charge *via* the Internet at http://pubs.acs.org.

REFERENCES AND NOTES

1. Decher, G.; Hong, J.-D.; Schmitt, J. Buildup of Ultrathin Multilayer Films by a Self-Assembly Process: III. Consecutively Alternating Adsorption of Anionic and Cationic Polyelectrolytes on Charged Surfaces. *Thin Solid Films* **1992**, *210/211*, 831–835.
2. Decher, G. Fuzzy Nanoassemblies: Toward Layered Polymeric Multicomposites. *Science* **1997**, *277*, 1232–1237.
3. Serizawa, T.; Matsukuma, D.; Nanameki, K.; Uemura, M.; Kurusu, F.; Akashi, M. Stepwise Preparation and Characterization of Ultrathin Hydrogels Composed of Thermoresponsive Polymers. *Macromolecules* **2004**, *37*, 6531–6536.
4. Glinel, K.; Sukhorukov, G. B.; Möhwald, H.; Khrenov, V.; Tauer, K. Thermosensitive Hollow Capsules Based on Thermoresponsive Polyelectrolytes. *Macromol. Chem. Phys.* **2003**, *204*, 1784–1790.
5. Jaber, J. A.; Schlenoff, J. B. Polyelectrolyte Multilayers with Reversible Thermal Responsivity. *Macromolecules* **2005**, *38*, 1300–1306.
6. Nayak, S.; Debord, S. B.; Lyon, L. A. Investigations into the Deswelling Dynamics and Thermodynamics of Thermoresponsive Microgel Composite Films. *Langmuir* **2003**, *19*, 7374–7379.
7. Nolan, C. M.; Serpe, M. J.; Lyon, L. A. Thermally Modulated Insulin Release from Microgel Thin Films. *Biomacromolecules* **2004**, *5*, 1940–1946.
8. Serpe, M. J.; Jones, C. D.; Lyon, L. A. Layer-by-Layer Deposition of Thermoresponsive Microgel Thin Films. *Langmuir* **2003**, *19*, 8759–8764.
9. Kozlovskaya, V.; Ok, S.; Sousa, A.; Libera, M.; Sukhishvili, S. A. Hydrogen-Bonded Polymer Capsules Formed by Layer-by-Layer Self-Assembly. *Macromolecules* **2003**, *36*, 8590–8592.
10. Quinn, J. F.; Caruso, F. Facile Tailoring of Film Morphology and Release Properties Using Layer-by-Layer Assembly of Thermoresponsive Materials. *Langmuir* **2004**, *20*, 20–22.
11. Quinn, J. F.; Caruso, F. Thermoresponsive Nanoassemblies: Layer-by-Layer Assembly of Hydrophilic−Hydrophobic Alternating Copolymers. *Macromolecules* **2005**, *38*, 3414–3419.
12. Wang, A.; Tao, C.; Cui, Y.; Duan, L.; Yang, Y.; Li, J. Assembly of Environmental Sensitive Microcapsules of PNIPAAm and Alginate Acid and Their Application in Drug Release. *J. Colloid Interface Sci.* **2009**, *332*, 271–279.
13. Maeda, Y. IR Spectroscopic Study on the Hydration and the Phase Transition of Poly(vinyl methyl ether) in Water. *Langmuir* **2001**, *17*, 1737–1742.
14. Yanul, N.; Kirsh, Y.; Anufrieva, E. Thermosensitive Water−Polymer Systems Studied by Luminescent Spectroscopy. *J. Therm. Anal. Calorim.* **2000**, *62*, 7–14.
15. Kharlampieva, E.; Kozlovskaya, V.; Tyutina, J.; Sukhishvili, S. A. Hydrogen-Bonded Multilayers of Thermoresponsive Polymers. *Macromolecules* **2005**, *38*, 10523–10531.
16. Ma, N.; Zhang, H. Y.; Song, B.; Wang, Z. Q.; Zhang, X. Polymer Micelles as Building Blocks for Layer-by-Layer Assembly: An Approach for Incorporation and Controlled Release of Water-Insoluble Dyes. *Chem. Mater.* **2005**, *17*, 5065–5069.
17. Ma, N.; Wang, Y.; Wang, Z.; Zhang, X. Polymer Micelles as Building Blocks for the Incorporation of Azobenzene: Enhancing the Photochromic Properties in Layer-by-Layer Films. *Langmuir* **2006**, *22*, 3906–3909.
18. Ma, N.; Wang, Y.; Wang, B.; Wang, Z.; Zhang, X. Interaction between Block Copolymer Micelles and Azobenzene-Containing Surfactants: From Coassembly in Water to Layer-by-Layer Assembly at the Interface. *Langmuir* **2007**, *23*, 2874–2878.
19. Liu, X.; Zhou, L.; Geng, W.; Sun, J. Layer-by-Layer-Assembled Multilayer Films of Polyelectrolyte-Stabilized Surfactant Micelles for the Incorporation of Noncharged Organic Dyes. *Langmuir* **2008**, *24*, 12986–12989.

20. Kang, E.; Lee, S. C.; Park, K. Layer-by-layer Assembly of Poly(lactic-co-glycolic acid)-bpoly(L-lysine) Copolymer Micelles. *Nanobiotechnology* **2007**, *3*, 96–103.
21. Qi, B.; Tong, X.; Zhao, Y. Layer-by-Layer Assembly of Two Different Polymer Micelles with Polycation and Polyanion Coronas. *Macromolecules* **2006**, *39*, 5714–5719.
22. Cho, J.; Hong, J.; Char, K.; Caruso, F. Nanoporous Block Copolymer Micelle/Micelle Multilayer Films with Dual Optical Properties. *J. Am. Chem. Soc.* **2006**, *128*, 9935–9942.
23. Biggs, S.; Sakai, K.; Addison, T.; Schmid, A.; Armes, S. P.; Vamvakaki, M.; Bütün, V.; Webbe, G. Layer-by-Layer Formation of Smart Particle Coatings Using Oppositely Charged Block Copolymer Micelles. *Adv. Mater.* **2007**, *19*, 247–250.
24. Sakai, K.; Webber, G. B.; Vo, C. D.; Wanless, E. J.; Vamvakaki, M.; Butun, V.; Armes, S. P.; Biggs, S. Characterization of Layer-by-Layer Self-Assembled Multilayer Films of Diblock Copolymer Micelles. *Langmuir* **2008**, *24*, 116–123.
25. Bo, Q.; Tong, X.; Zhao, Y.; Zhao, Y. A Micellar Route to Layer-by-Layer Assembly of Hydrophobic Functional Polymers. *Macromolecules* **2008**, *41*, 3562–3570.
26. Kim, B. S.; Park, S. W.; Hammond, P. T. Hydrogen-Bonding Layer-by-Layer-Assembled Biodegradable Polymeric Micelles as Drug Delivery Vehicles from Surfaces. *ACS Nano* **2008**, *2*, 386–392.
27. Webber, G. B.; Wanless, E. J.; Armes, S. P.; Tang, Y.; Li, Y.; Biggs, S. Nano-anemones: Stimulus-Responsive Copolymer-Micelle Surfaces. *Adv. Mater.* **2004**, *16*, 1794–1798.
28. Kim, B. S.; Lee, H. I.; Min, Y.; Poon, Z.; Hammond, P. T. Hydrogen-Bonded Multilayer of pH-Responsive Polymeric Micelles with Tannic Acid for Surface Drug Delivery. *Chem. Commun.* **2009**, 4194–4196.
29. Dimitrov, I.; Trzebicka, B.; Müller, A. H. E.; Dworak, A.; Tsvetanov, C. B. Thermosensitive Water-Soluble Copolymers with Doubly Responsive Reversibly Interacting Entities. *Prog. Polym. Sci.* **2007**, *32*, 1275–1343.
30. Jiang, X.; Ge, Z.; Xu, J.; Liu, H.; Liu, S. Fabrication of Multiresponsive Shell Cross-Linked Micelles Possessing pH-Controllable Core Swellability and Thermo-Tunable Corona Permeability. *Biomacromolecules* **2007**, *8*, 3184–3192.
31. Li, D.; He, Q.; Li, J. Smart Core/Shell Nanocomposites: Intelligent Polymers Modified Gold Nanoparticles. *Adv. Colloid Interface Sci.* **2009**, *149*, 28–38.
32. Wan, D. C.; Satoh, K.; Kamigaito, M.; Okamoto, Y. Xanthate-Mediated Radical Polymerization of *N*-Vinylpyrrolidone in Fluoroalcohols for Simultaneous Control of Molecular Weight and Tacticity. *Macromolecules* **2005**, *38*, 10397–10405.
33. Fujishige, S.; Kubota, K.; Ando, I. Phase Transition of Aqueous Solutions of Poly(*N*-isopropylacrylamide) and Poly(*N*-isopropylmethacrylamide). *J. Phys. Chem.* **1989**, *93*, 3311–3313.
34. Winnik, F. M. Fluorescence Studies of Aqueous Solutions of Poly(*N*-isopropylacrylamide) below and above Their LCST. *Macromolecules* **1990**, *23*, 233–242.
35. Dhara, D.; Chatterji, P. R. Phase Transition in Linear and Cross-Linked Poly(*N*-isopropylacrylamide) in Water: Effect of Various Types of Additives. *J. Macromol. Sci., Rev. Macromol. Chem. Phys.* **2000**, *C40*, 51–68.
36. Schild, H. G.; Tirrell, D A.; Schild, H. G.; Tirrell, D. A. Microcalorimetric Detection of Lower Critical Solution Temperatures in Aqueous Polymer Solutions. *J. Phys. Chem.* **1990**, *94*, 4352–4356.
37. Suwa, K.; Yamamoto, K.; Akashi, M.; Takano, K.; Tanaka, N.; Kunugi, S. Effects of Salt on the Temperature and Pressure Responsive Properties of Poly(*N*-vinylisobutyramide) Aqueous Solutions. *Colloid Polym. Sci.* **1998**, *276*, 529–533.
38. Freitag, R.; Garret-Flaudy, F. Salt Effects on the Thermoprecipitation of Poly-(*N*-isopropylacrylamide) Oligomers from Aqueous Solution. *Langmuir* **2002**, *18*, 3434–3440.
39. Zhang, Y.; Furyk, S.; Bergbreiter, D. E.; Cremer, P. S. Specific Ion Effects on the Water Solubility of Macromolecules: PNIPAM and the Hofmeister Series. *J. Am. Chem. Soc.* **2005**, *127*, 14505–14510.
40. Kozlovskaya, V.; Kharlampieva, E.; Mansfield, M. L.; Sukhishvili, S. A. Poly(methacrylic acid) Hydrogel Films and Capsules: Response to pH and Ionic Strength, and Encapsulation of Macromolecules. *Chem. Mater.* **2006**, *18*, 328–336.
41. Jin, S.; Liu, M.; Chen, S.; Gao, C. Synthesis, Characterization, and the Rapid Response Property of the Temperature Responsive PVP-g-PNIPAM Hydrogel. *Eur. Polym. J.* **2008**, *44*, 2162–2170.
42. Nguyen, P. M.; Zacharia, N. S.; Verploegen, E.; Hammond, P. T. Extended Release Antibacterial Layer-by-Layer Films Incorporating Linear-Dendritic Block Copolymer Micelles. *Chem. Mater.* **2007**, *19*, 5524–5530.
43. Sukhishvili, S. A.; Granick, S. Layered, Erasable Polymer Multilayers Formed by Hydrogen-Bonded Sequential Self-Assembly. *Macromolecules* **2002**, *35*, 301–310.
44. Pristinski, D.; Kozlovskaya, V.; Sukhishvili, S. A. Determination of Film Thickness and Refractive Index in One Measurement of Phase-Modulated Ellipsometry. *J. Opt. Soc. Am. A.* **2006**, *23*, 2639–2644.
45. Kozlovskaya, V.; Yakovlev, S.; Libera, M.; Sukhishvili, S. Surface Priming and the Self-Assembly of Hydrogen-Bonded Multilayer Capsules and Films. *Macromolecules* **2005**, *38*, 4828–4836.
46. Kalyanasundaram, K.; Thomas, J. K. Environmental Effects on Vibronic Band Intensities in Pyrene Monomer Fluorescence and Their Application in Studies of Micellar Systems. *J. Am. Chem. Soc.* **1977**, *99*, 2039–2044.
47. Philippova, O. E.; Karybiants, N. S.; Starodubtzev, S. G. Conformational Changes of Hydrogels of Poly(methacrylic acid) Induced by Interaction with Poly(ethylene glycol). *Macromolecules* **1994**, *27*, 2398–2401.
48. Lynch, I.; de Gregorio, P.; Dawson, K. A. Simultaneous Release of Hydrophobic and Cationic Solutes from Thin-Film "Plum-Pudding" Gels: A Multifunctional Platform for Surface Drug Delivery. *J. Phys. Chem. B* **2005**, *109*, 6257–6261.
49. He, Q.; Song, W.; Möhwald, H.; Li, J. Hydrothermal-Induced Structure Transformation of Polyelectrolyte Multilayers: From Nanotubes to Capsules. *Langmuir* **2008**, *24*, 5508–5513.
50. Wu, C.; Zhou, S. Laser Light Scattering Study of the Phase Transition of Poly(*N*-isopropylacrylamide) in Water. 1. Single Chain. *Macromolecules* **1995**, *28*, 8381–8387.